Magazine of Civil Engineering

ISSN 2712-8172

journal homepage: http://engstroy.spbstu.ru/

Research article

UDC 539.3

DOI: 10.34910/MCE.113.14

# Physically nonlinear shell deformation based on three-dimensional finite elements

***Yu.V. Klochkov*** [a], ***A.P. Nikolaev*** [a], ***O.V. Vakhnina*** [a], ***T.A. Sobolevskaya*** [a] ✉, ***M.Yu. Klochkov*** [b]

[a] *Volgograd State Agricultural University, Volgograd, Russian Federation*

[b] *Lomonosov Moscow State University, Moscow, Russian Federation*

✉ *moonway13@rambler.ru*

**Keywords:** physical nonlinearity, three-dimensional finite element, shell, stress increment deviator, strain increment deviator

**Abstract.** The aim of the study is to determine the stress-strain state of the shell under step loading beyond the elastic limit. At the loading step, relations between strain increments and stress increments are obtained without accepting the hypothesis of a straight normal. For the numerical implementation of the algorithm in the calculation of the shell without using a straight normal, a prismatic finite element has been developed. We consider the physically nonlinear deformation of the shell, an arbitrary point of which is represented by a radius vector defined by the curvilinear coordinates of the reference surface and the distance from the reference surface to the point under consideration. By differentiating the radius-vector function, the basis vectors of the point under consideration are determined, the scalar products of which are the components of its metric tensor. The increments of deformations at the loading step are defined as the differences of the corresponding components of the metric tensors. The defining equations at the loading step are obtained in two versions. In the first version, they are determined by differentiating the stress functions of the deformation theory of plasticity, which are obtained on the basis of dividing deformations into elastic and plastic parts using the hypothesis of material incompressibility during plastic deformation. In the second version, they are obtained without using the operation of dividing the strain increments into elastic and plastic parts on the basis of the proposed hypothesis that the components of the deviator of the stress increments are proportional to the components of the deviator of the increments of deformations. For the numerical implementation, a three-dimensional prismatic finite element with a triangular base was used for nodal unknowns in the form of displacements and their first derivatives with respect to curved coordinates. The correctness of the proposed variant of obtaining physically nonlinear defining equations at the loading step of the deformable shell is confirmed by a numerical example. On the example of calculating a cylindrical shell under the action of internal pressure, clamped at one end and free at the other, the values of normal stresses in the embedment turned out to be approximately 14% lower in the case of using the proposed variant of obtaining the constitutive equations at the loading step. The developed algorithm for determining the stress-strain state in the physically nonlinear deformation of elements of technospheric objects can be used in the practice of engineering calculations.

**Funding:** The study was carried out with the financial support of the Russian Foundation for Basic Research and the Administration of the Volgograd Region in the framework of the research project No. 19-41-340005 r_ a.

**Citation:** Klochkov, Yu.V., Nikolaev, A.P., Vakhnina, O.V., Sobolevskaya, T.A., Klochkov, M.Yu. Physically nonlinear shell deformation based on three-dimensional finite elements. Magazine of Civil Engineering. 2022. 113(5). Article No. 11314. DOI: 10.34910/MCE.113.14

# 1. Introduction

Currently, technospheric objects are subject to rather stringent requirements to minimize their material consumption, without reducing the criterion of their strength, stability, durability, etc. The above requirements are fully met by shell-type structures with curved surfaces. The analysis of the stress-strain state (SSS) of such objects by classical analytical methods of calculation is difficult, especially in a nonlinear setting. The theory of the stress-strain state of a solid has received quite sufficient development [1–5]. To solve the problems of strength of objects of engineering practice, approximate calculation methods were developed both in a linear formulation [6–10] and in a nonlinear one [11–15]. Due to the complexity of solving the equations of deformation mechanics as applied to specific elements of engineering objects, the task of developing numerical methods for determining the stress-strain state has become urgent [16–20]. Among the numerical methods for calculating the constituent parts of engineering objects, the finite element method (FEM) has become widespread [20–22]. It has been applied to cylindrical shells of circular and elliptical sections [13, 14], as well as to plates and shells with finite deformations [15, 23, 24]. FEM was also widely used to calculate nonlinear elastic bodies and shells taking into account the Kirchhoff hypothesis [25–29]. Composite shells were calculated based on the FEM [30–33]. Volumetric finite elements were also used to calculate the shells without taking into account Kirchhoff's hypothesis [34–37]. Volumetric finite elements were used to calculate elastic and inelastic solids based on the method of virtual components [38, 39].

In the case of deformation of shell structures under various combinations of loads, it becomes possible for zones of significant stress concentrations to appear, in which the relationships between stresses and deformations become nonlinear. When solving problems of this class, the method of step loading [36] is widely used to obtain the governing physically nonlinear equations at the loading step, the method of decomposing the increments of deformations into elastic and plastic parts is used [37, 38].

When analyzing the SSS of shells of arbitrary configuration and thickness, the most promising are three-dimensional sampling elements without reduction to two-dimensional ones based on any hypothesis. Despite the wide range of computing systems of foreign and domestic production, the problem of improving the finite element algorithms for analyzing the SSS of technospheric shell-type objects based on three-dimensional discretization elements, taking into account the elastic-plastic stage of the material used, remains very urgent.

In this paper, at the loading step, an algorithm for the formation of the stiffness matrix of a prismatic discretization element is presented, intended for calculating structures from shells of arbitrary thickness and configuration, taking into account the physical nonlinearity of the material used. A distinctive feature of the study is the developed method for obtaining the constitutive equations at the loading step based on the hypothesis that the components of the deviator of the deformation increments are proportional to the components of the deviator of the stress increments without dividing the increments of deformations into elastic and plastic parts.

When implementing the proposed hypothesis, the proportionality coefficient of the constitutive equations turned out to be a function of the chord modulus of the material deformation diagram, which opens up prospects for using the constitutive equations obtained by this method even in the presence of unloading zones of the calculated structures.

# 2. Methods

The reference surface, which is the curvilinear boundary of the object under study, is determined by the radius vector [40] (Fig. 1).

$$\vec{R}^0 = x\left(\theta^1, \theta^2\right)\vec{i} + y\left(\theta^1, \theta^2\right)\vec{j} + z\left(\theta^1, \theta^2\right)\vec{k}, \quad (1)$$

where $\vec{i}$, $\vec{j}$, $\vec{k}$ are unit vectors of the Cartesian coordinate system, $\theta^\rho$ $(\rho = 1, 2)$ are curvilinear coordinates of the reference surface.

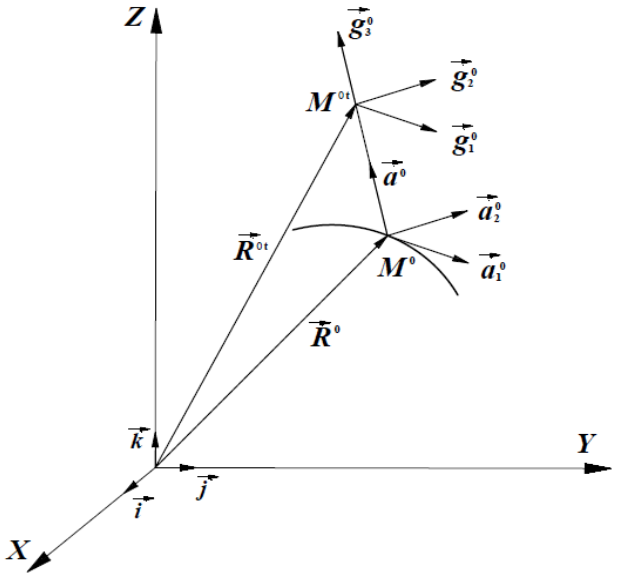


**Figure 1. Geometry of the shell: – an arbitrary point of the reference surface of the shell; – arbitrary point of the shell.**

The position of an arbitrary point $M^{0t}$ of the object located at a distance of $t$, measured along the normal to the reference surface, is determined by the radius vector of the form

$$\vec{R}^{0t} = \vec{R}^{0} + t\vec{\alpha}^{0}, \tag{2}$$

where $\vec{a}^{0} = \vec{a}_1^{0} \times \vec{a}_2^{0} \Big/ \left|\vec{a}_1^{0} \times \vec{a}_2^{0}\right|$ is the unit vector of the normal to the reference surface [41]; $\vec{a}_1^{0} = \vec{R}_{,\theta^1}^{0}$; $\vec{a}_2^{0} = \vec{R}_{,\theta^2}^{0}$. Here and below, the comma means the operation of differentiation by the corresponding coordinate, for example, $\theta^{\rho}\ (\rho = 1, 2)$.

The basis vectors of point $M^{0t}$ are determined by differentiating (2) with respect to $\theta^{\rho}$ and $t$.

$$\vec{g}_1^{0} = \vec{R}_{,\theta^1}^{0t}; \ldots \vec{g}_2^{0} = \vec{R}_{,\theta^2}^{0t}; \ldots \vec{g}_3^{0} = \vec{R}_{,t}^{0t}. \tag{3}$$

1. or in matrix form

$$\left\{\vec{g}^{0}\right\} = [l]\left\{\vec{i}\right\}; \ \left\{\vec{i}\right\} = [l]^{-1}\left\{\vec{g}^{0}\right\}, \tag{4}$$

where $\left\{\vec{g}^{0}\right\} = \left\{\vec{g}_1^{0}\vec{g}_2^{0}\vec{g}_3^{0}\right\}$, $\left\{\vec{i}\right\}^{T} = \left\{\vec{i}\ \vec{j}\ \vec{k}\right\}$.

2. Differentiation (3) with allowance for (4) determines the derivatives of the basis vectors by the components in this basis

$$\left\{\vec{g}_{,i}^{0}\right\} = [Z_i][l]^{-1}\left\{\vec{g}^{0}\right\} = [m_i]\left\{\vec{g}^{0}\right\}, \tag{5}$$

where $\left\{\vec{g}_{,i}^{0}\right\}^{T} = \left\{\vec{g}_{1,i}^{0}\vec{g}_{2,i}^{0}\vec{g}_{3,i}^{0}\right\}; \ \left(i = \theta^1, \theta^2, t\right)$.

When studying the stress-strain state of technospheric objects in a nonlinear formulation, a step-by-step loading procedure is usually used, during which an arbitrary point of object $M^{0t}$ will move to point $M^{t}$ in $j$ loading steps, and to point $M^{*t}$ in the $(j+1)^{\text{th}}$ loading step.

The positions of points $M^{t}$ and $M^{*t}$ are determined by the corresponding radius vectors

$$\vec{R}^{t} = \vec{R}^{0t} + \vec{V}; \ \vec{R}^{*t} = \vec{R}^{t} + \vec{W}, \tag{6}$$

where $\vec{V} = v^i \vec{g}_i^0$ and $\vec{W} = w^i \vec{g}_i^0$ are the total and step vectors of displacement of point $M^{0t}$.

The vectors of bases at points $M^t$ and $M^{0t}$ can be determined by differentiating (6) with respect to $\theta^\rho$ and $t$.

$$\begin{aligned}\vec{g}_1 = \vec{R}^t_{,\theta^1} = \vec{g}_1^0 + \vec{V}_{,\theta^1}; \ldots \vec{g}_2 = \vec{R}^t_{,\theta^2} = \vec{g}_2^0 + \vec{V}_{,\theta^2}; \ldots \vec{g}_3 = \vec{R}^t_{,t} = \vec{g}_3^0 + \vec{V}_{,t};\\ \vec{g}_1^* = \vec{R}^{*t}_{,\theta^1} = \vec{g}_1 + \vec{W}_{,\theta^1}; \ldots \vec{g}_2^* = \vec{R}^{*t}_{,\theta^2} = \vec{g}_2 + \vec{W}_{,\theta^2}; \ldots \vec{g}_3^* = \vec{R}^{*t}_{,t} = \vec{g}_3 + \vec{W}_{,t}.\end{aligned} \quad (7)$$

The covariant components of the metric tensors at points $M^{0t}$, $M^t$, and $M^{*t}$ can be obtained by scalar products of vectors (3), (7).

$$g^0_{mn} = \vec{g}^0_m \cdot \vec{g}^0_n; \ g_{mn} = \vec{g}_m \cdot \vec{g}_n; \ g^*_{mn} = \vec{g}^*_m \cdot \vec{g}^*_n. \quad (8)$$

The covariant components of the deformation tensor at point $M^t$ in $j$ loading steps and the increment tensor at the $(j+1)^{\text{th}}$ loading step at point $M^{*t}$ can be calculated using the classical relations of continuum mechanics [42]

$$\varepsilon_{mn} = 0.5 \cdot \left( g_{mn} - g^0_{mn} \right); \ \Delta\varepsilon_{mn} = 0.5 \cdot \left( g^*_{mn} - g_{mn} \right), \quad (9)$$

which are represented in matrix form

$$\underset{6\times1}{\{\varepsilon\}} = \underset{6\times3}{[L_1]} \underset{3\times1}{\{v\}}; \ \underset{6\times1}{\{\Delta\varepsilon\}} = \underset{6\times3}{[L_2]} \underset{3\times1}{\{w\}}, \quad (10)$$

where $\underset{1\times6}{\{\varepsilon\}^T} = \{\varepsilon_{11}\varepsilon_{22}\varepsilon_{33}2\varepsilon_{12}2\varepsilon_{13}2\varepsilon_{23}\}$; $\underset{1\times6}{\{\Delta\varepsilon\}^T} = \{\Delta\varepsilon_{11}\Delta\varepsilon_{22}\Delta\varepsilon_{33}2\Delta\varepsilon_{12}2\Delta\varepsilon_{13}2\Delta\varepsilon_{23}\}$;

$\underset{1\times3}{\{v\}^T} = \{v^1 v^2 v^3\}$; $\underset{1\times3}{\{w\}^T} = \{w^1 w^2 w^3\}$; $\underset{6\times3}{[L_1]}$ and $\underset{6\times3}{[L_2]}$ matrices of algebraic and differential operators.

3. Matrix of elastic-plastic deformation at the $(j+1)^{\text{th}}$ step of loading

At the $(j+1)^{\text{th}}$ loading step, it is necessary to have a relationship between the stress increment tensor and the strain increment tensor.

To obtain ratios in a curvilinear coordinate system between the components of stress and strain tensors, the hypothesis of proportionality of the stress deviator components to the strain deviator components is used [43]

$$\sigma^{mn} - \frac{1}{3} g^{mn} I_1(\sigma) = \frac{2}{3} E_c \left( \varepsilon^{mn} - \frac{1}{3} g^{mn} I_1(\varepsilon) \right), \quad (11)$$

where $\sigma^{mn}$ is contravariant component of the stress tensor; $g^{mn}$ is contravariant component of the metric tensor; $\varepsilon^{mn} = g^{mi} g^{nj} \varepsilon_{ij}$ is contravariant component of the strain tensor; $I_1(\varepsilon) = g^{ij} \varepsilon_{ij} = g_{ij} \varepsilon^{ij}$ is the first invariant of the strain tensor; $I_1(\sigma) = \sigma^{ij} g_{ij} = \sigma_{ij} g^{ij}$ is the first invariant of the stress tensor; $E_c$ is secant module of the deformation diagram.

The relationship between the first invariants of the stress and strain tensors is [43]

$$I_1(\sigma) = \frac{E}{1-2\nu} I_1(\varepsilon) = K \cdot I_1(\varepsilon), \quad (12)$$

where $E$ is the modulus of elasticity of the material; $\nu$ is coefficient of transverse deformation.

Using (12) from (11), expressions for the contravariant components of the stress tensor are determined

$$\sigma^{mn} = \frac{2}{3} E_c g^{mi} g^{nj} \varepsilon_{ij} + \frac{1}{3} g^{mn} I_1(\varepsilon)\left( K - \frac{2}{3} E_c \right). \tag{13}$$

The relationships between the increments of the stress tensor components and the increments of the components of the deformation tensor are determined by differentiation (13)

$$\Delta\sigma^{mn} = \frac{\partial \sigma^{mn}}{\partial \varepsilon_{ij}} \Delta \varepsilon_{ij}, \tag{14}$$

or in matrix form

$$\underset{6\times1}{\{\Delta\sigma\}} = \underset{6\times6}{\left[ C_1^{\Pi} \right]} \underset{6\times1}{\{\Delta\varepsilon\}}, \tag{15}$$

where $\left\{\Delta\sigma^{mn}\right\}^T = \left\{\Delta\sigma^{11}\Delta\sigma^{22}\Delta\sigma^{33}\Delta\sigma^{12}\Delta\sigma^{13}\Delta\sigma^{23}\right\}$.

The implementation of relations (14) in a three-dimensional formulation involves a significant amount of analytical calculations due to the variability of the components of the metric tensors, which significantly complicates the programming procedure. Therefore, in this work, we propose a layout of the constitutive equations at the $(j+1)^{\text{th}}$ step of loading based on the proposed hypothesis of proportionality of the components of the deviator of the stress increments to the components of the deviator of the increments of deformations, according to which the following expression can be written

$$\Delta\sigma^{mn} - \frac{1}{3} g^{mn} I_1(\Delta\sigma) = \frac{2}{3} E_x \left( \Delta\varepsilon^{mn} - \frac{1}{3} g^{mn} I_1(\Delta\varepsilon) \right), \tag{16}$$

where $\Delta\sigma^{mn}$ is contravariant component of the stress increment tensor; $\Delta\varepsilon^{mn} = g^{mi} g^{nj} \Delta\varepsilon_{ij}$ is contravariant component of the strain increment tensor; $I_1(\Delta\varepsilon) = g^{ij}\Delta\varepsilon_{ij} = g_{ij}\Delta\varepsilon^{ij}$ is the first invariant of the strain increment tensor; $I_1(\Delta\sigma) = \Delta\sigma^{ij} g_{ij} = \Delta\sigma_{ij} g^{ij}$ is the first invariant of the stress increment tensor; $E_x$ is chordal module of the material deformation diagram.

Taking the relationship between the first invariants $I_1(\Delta\sigma)$ and $I_1(\Delta\varepsilon)$ according to (12), based on (16), the governing equations at the loading step can be written in the form

$$\Delta\sigma^{mn} = \frac{2}{3} E_x g^{mi} g^{nj} \Delta\varepsilon_{ij} + \frac{1}{3} g^{mn} I_1(\Delta\varepsilon)\left( K - \frac{2}{3} E_x \right), \tag{17}$$

which are represented in matrix form

$$\underset{6\times1}{\{\Delta\sigma\}} = \underset{6\times6}{\left[ C_2^{\Pi} \right]} \underset{6\times1}{\{\Delta\varepsilon\}}. \tag{18}$$

4. Stiffness matrix of the prismatic discretization element at the $(j+1)^{\text{th}}$ loading step

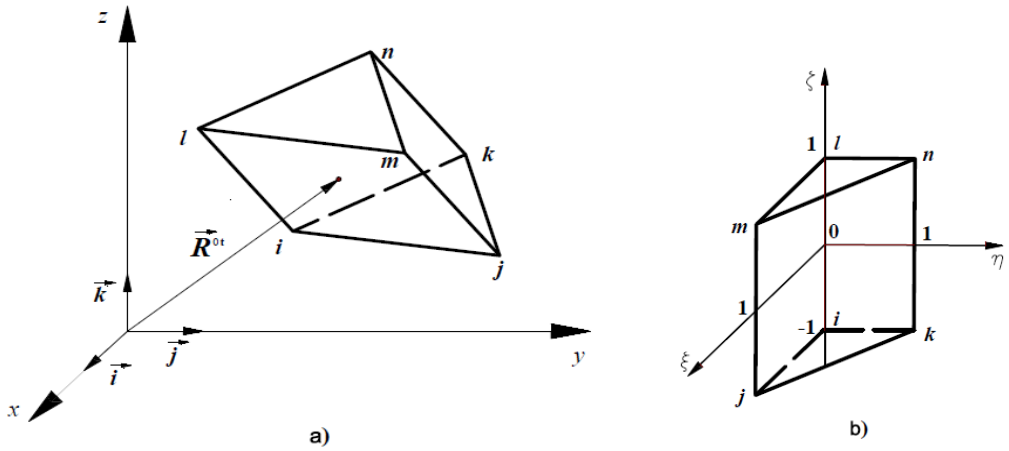


**Figure 2. Finite element geometry: in the global coordinate system; b) in the local coordinate system.**

A prismatic fragment with triangular bases with nodes $i$, $j$, $k$ (lower base) and $l$, $m$, $n$ (upper base) (Fig. 2a) was chosen as the sampling element for the investigated technospheric object of the shell type. To perform numerical integration, the prismatic fragment was mapped onto a local prism with a triangular base in the form of a right-angled triangle with local coordinates varying within $0 \le \xi,\ \eta \le 1$ and with a local coordinate in height varying within $-1 \le \zeta \le 1$ (Fig. 2b). The nodal variable parameters of this element are the increments of the displacement vector components and their first-order partial derivatives. The columns of the required step nodal unknowns in the local $\xi$, $\eta$, $\zeta$ and global $\theta^1, \theta^2, t$ coordinate systems can be represented in the following form

$$\underset{1\times 72}{\left\{W^L\right\}^T} = \left\{ \underset{1\times 24}{\left\{w^{1L}\right\}^T}\ \underset{1\times 24}{\left\{w^{2L}\right\}^T}\ \underset{1\times 24}{\left\{w^{3L}\right\}^T} \right\}; \tag{19}$$

$$\underset{1\times 72}{\left\{W^G\right\}^T} = \left\{ \underset{1\times 24}{\left\{w^{1G}\right\}^T}\ \underset{1\times 24}{\left\{w^{2G}\right\}^T}\ \underset{1\times 24}{\left\{w^{3G}\right\}^T} \right\}, \tag{20}$$

where $\underset{1\times 24}{\left\{q^L\right\}^T} = \left\{q^i q^j q^k q^l q^m q^n q^i_{,\xi} \dots q^n_{,\xi} q^i_{,\eta} \dots q^n_{,\eta} q^i_{,\zeta} \dots q^n_{,\zeta}\right\}$;

$\underset{1\times 24}{\left\{q^G\right\}^T} = \left\{q^i \dots q^n q^i_{,\theta^1} \dots q^n_{,\theta^1} q^i_{,\theta^2} \dots q^n_{,\theta^2} q^i_{,t} \dots q^n_{,t}\right\}$; $q$ is understood as the component of the step motion vector $\vec{w} = w^1\vec{a}_1^0 + w^2\vec{a}_2^0 + w^3\vec{a}^0$.

When approximating the components of the displacement vector at the loading step, we used the products of two-dimensional polynomials of the third degree in the planes of triangular bases and Hermite polynomials of the third degree in the direction of the height of the local prism

$$\left\{w\right\} = \left[A\right]\left\{W^L\right\} = \left[A\right]\left[P_R\right]\left\{W^G\right\}, \tag{21}$$

where $\left[P_R\right]$ is transformation matrix between columns of nodal unknowns in local and global coordinate systems.

Taking into account (21), the strain increments are determined by the following expression

$$\left\{\Delta\varepsilon\right\} = \left[L_2\right]\left[A\right]\left\{W^L\right\} = \left[B\right]\left[P_R\right]\left\{W^G\right\}. \tag{22}$$

For the arrangement of the stiffness matrix and the column of nodal forces of the prismatic discretization element at the $(j+1)^{\text{th}}$ loading step, the Lagrange functional was used

$$\Phi_L = \int_V \left\{\Delta\varepsilon\right\}^T \left(\left\{\sigma\right\} + \left\{\Delta\sigma\right\}\right) \mathrm{d}V - \int_S \left\{w\right\}^T \left(\left\{P\right\} + \left\{\Delta P\right\}\right) \mathrm{d}S, \tag{23}$$

where $\{P\}$; $\{\Delta P\}$ are columns of the external load in $j$ loading steps and increments of this load at the $(j+1)^{\text{th}}$ loading step; $\{\sigma\}$, $\{\Delta\sigma\}$ are columns containing contravariant components of stress tensors accumulated over $j$ loading steps and increments of these stresses at the $(j+1)^{\text{th}}$ loading step; $V$ is volume; $S$ is load application surface.

Functional (23), taking into account (22), can be transformed to the form

$$\begin{aligned}\Phi_L = &\left\{W^G\right\}^T \left[P_R\right]^T \int\limits_V \left[B\right]^T \left\{\sigma^{mn}\right\} \mathrm{d}V + \\ &+\left\{W^G\right\}^T \left[P_R\right]^T \int\limits_V \left[B\right]^T \left[C_{II}\right]\left[B\right]\mathrm{d}V\left[P_R\right]\left\{W^G\right\} - \\ &-\left\{W^G\right\}^T \left[P_R\right]^T \int\limits_S \left[A\right]^T \left\{P\right\}\mathrm{d}S - \left\{W^G\right\}^T \left[P_R\right]^T \int\limits_S \left[A\right]^T \left\{\Delta P\right\}\mathrm{d}S.\end{aligned} \tag{24}$$

By minimizing (24) by $\left\{w^G\right\}^T$, one can obtain the following matrix expression

$$\left[K\right]\left\{W^G\right\} = \left\{f\right\} - \left\{R\right\}, \tag{25}$$

where $\left[K\right] = \left[P_R\right]^T \int\limits_V \left[B\right]^T \left[C_{II}\right]\left[B\right]\mathrm{d}V\left[P_R\right]$ is stiffness matrix of the prismatic sampling element at the $(j+1)^{\text{th}}$ loading step; $\left\{f\right\} = \left[P_R\right]^T \int\limits_S \left[A\right]^T \left\{\Delta P\right\}\mathrm{d}S$ is column of nodal forces of the sampling element at the $(j+1)^{\text{th}}$ loading step; $\left\{R\right\} = \left(\left[P_R\right]^T \int\limits_V \left[B\right]^T \left\{\sigma\right\}\mathrm{d}V - \left[P_R\right]^T \int\limits_S \left[A\right]^T \left\{P\right\}\mathrm{d}S\right)$ is Newton-Raphson correction.

## 3. Results and Discussion

In order to verify the developed algorithm, a test problem was solved to determine the stress-strain state of a circular cylinder rigidly clamped along the right end and having a left end free of fixings (Fig. 3). The cylinder was loaded with an internal pressure of intensity $q = 3.5$ MPa. Geometrical dimensions of the cylinder: generatrix length $L = 0.8$ m; the radius of the inner surface of the cylinder is $R = 0.895$ m; wall thickness $t = 0.01$ m. Duralumin alloy $E = 7.5 \cdot 10^4$ MPa was used as a material; $\nu = 0.32$. The deformation diagram was selected with linear hardening determined by the formula

$$\sigma_i = 18087\left(\varepsilon_i - \varepsilon_i^T\right) + \sigma_i^T, \tag{26}$$

where $\varepsilon_i^T = 0.00295$ is the intensity of deformations corresponding to the yield point; $\sigma_i^T = 200$ MPa is stress intensity corresponding to the yield point.

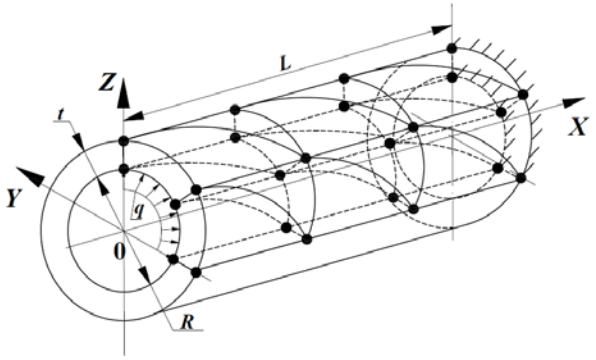


**Figure 3. Design scheme of the shell.**

Along the generatrix, the cylinder was divided into 25 finite elements. The shell was crushed into 8 sampling points along the thickness.

The results of finite element calculations are summarized in a table, which shows the values of "physical" normal stresses on the outer $\sigma^{out}$ and inner $\sigma^{in}$ surfaces of the cylinder in a rigid embedment and at the free end, depending on the number of loading steps.

It should be noted that the stress values obtained using the constitutive relations according to (14) and (16) turned out to be quite close.

***Table 1. Values of normal stresses in the rigid termination and at the free end of the cylinder.***

| Cross section | Stress, MPa | Number of loading steps | | | | Analytical stress values |
|---|---|---|---|---|---|---|
| | | 12 | 22 | 32 | 42 | |
| Rigid termination | $\sigma_{11}^{in}$ | 421.4 | 436.1 | 434.7 | 434.0 | – |
| | $\sigma_{11}^{out}$ | –440.1 | –436.5 | –433.6 | –432.7 | – |
| | $\sigma_{22}^{in}$ | 198.3 | 205.2 | 204.6 | 204.2 | – |
| | $\sigma_{22}^{out}$ | –207.1 | –205.4 | –204.0 | –203.6 | – |
| Free end | $\sigma_{11}^{in}$ | 0.003 | 0.003 | 0.002 | 0.0019 | 0.000 |
| | $\sigma_{11}^{out}$ | -0.003 | 0.000 | 0.001 | 0.001 | 0.000 |
| | $\sigma_{22}^{in}$ | 310.6 | 313.8 | 314.9 | 315.4 | 315.0 |
| | $\sigma_{22}^{out}$ | 317.3 | 315.4 | 314.8 | 314.5 | 315.0 |
| | $\sigma_{33}^{in}$ | –3.50 | –3.50 | –3.50 | –3.50 | –3.50 |
| | $\sigma_{33}^{out}$ | 0.003 | 0.003 | 0.003 | 0.004 | 0.000 |

Analysis of the numerical values of the stresses presented in Table 1 shows that there is a stable convergence of the computational process with an increase in the number of loading steps. The numerical values of the stresses at the free end of the cylinder practically coincide with the values obtained from the static equations. The meridional stresses $(\sigma_{11})$ at the end of the cylinder must be zero, because the external load, represented by the internal pressure $q$, acts along the normal to the inner surface of the cylinder and its projection onto the generatrix of the cylinder is zero. Hoop stresses $(\sigma_{22})$ can be obtained from the equilibrium condition of $\sigma_{22} = \frac{qR}{t} = \frac{3.5 \cdot 0.9}{0.01} = 315.0$ MPa. The stresses acting along the normal to the inner surface must coincide in absolute value with the intensity of the inner pressure, i.e. $\sigma_{33} = -q = -3.5$ MPa.

Analyzing the numerical values of normal stresses $\sigma_{11}$ in a rigid termination, it can be noted that they correspond to the condition of static equilibrium, namely: the sum of internal longitudinal forces should be zero, since there are no external longitudinal forces. The sum of internal longitudinal forces can be determined by calculating the areas of the diagrams of compressive and tensile stresses $\sigma_{11}$, approximately taking the area in the form of the sums of triangular and trapezoidal fragments (Fig. 4).

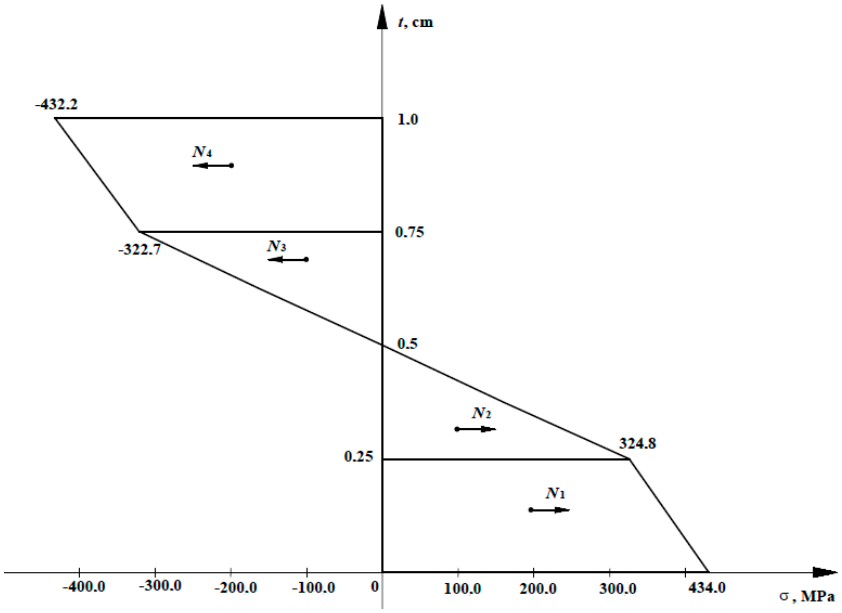


**Figure 4. Stress diagram $\sigma_{11}$ in a rigid termination with the number of steps $n_s = 42$**

The total tensile force is $N_t = N_1 + N_2 = 1354.5$ kN and the total compressive force is $N_c = N_3 + N_4 = 1347.0$ kN.

The difference between $N_t$ and $N_c$ is negligible (about 0.16 %).

In the numerical implementation of the developed algorithm on the considered test problem, a calculation was performed based on the relationships between stress increments and strain increments obtained by differentiating the governing equations of the deformation theory of plasticity (10) in accordance with formula (11). The use of this differentiation approach is widespread [44, 45]. The numerical values of normal stresses in a rigid seal based on formula (11) turned out to be 15.6 % less for $\sigma_{11}^{in}$ and 14.2 % less for hoop stresses $\sigma_{22}^{in}$.

Fig. 5 shows graphs showing changes in normal stresses $\sigma_{11}$ and $\sigma_{22}$ in a rigid seal on the inner $\sigma^{in}$ and outer $\sigma^{out}$ surfaces of the cylinder, depending on the number of prismatic elements along the generatrix of the cylinder. As can be seen from Fig. 5, there is a stable convergence of the computational process when the discretization grid is refined, which is an additional criterion for the adequacy of the developed calculation algorithm.


**Figure 5. Stresses $\sigma_{11}$ and $\sigma_{22}$ in a rigid termination depending on the number of finite elements along the generatrix.**

# 4. Conclusion

Based on the research performed, the following conclusions can be drawn:

1. The difference in the numerical values of the normal stresses in the embedding of the cylindrical shell from the effect of internal pressure, obtained on the basis of the constitutive equations (10) and (11), turned out to differ by about 14 %. Consequently, in the case of elastic-plastic deformation, it is physically more reasonable to obtain the governing equations between stress increments and strain increments on the basis of the proposed hypothesis that the components of the deviator of the stress increments are proportional to the components of the deviator of the increments of deformations.

2. For strength calculations of shells of various shapes and thicknesses, it is preferable to use the developed volumetric finite element without using additional hypotheses about deformation along the thickness of the shell structures.

3. A numerical example confirmed the accuracy of determining the parameters of strength during deformation beyond the elastic limit, sufficient for solving shell-type engineering objects.

## References


1. Novozhilov, V.V. Teoriya tonkikh obolochek [Theory of thin shells]. St. Petersburg: Publishing House of the St. Petersburg University, 2010. 378 p. (rus)
2. Kabrits, S.A., Mikhailovsky, E.I., Tovstik, P.E., Chernykh, K.F., Shamina, V.A. Obshchaya nelineynaya teoriya uprugikh obolochek [General nonlinear theory of elastic shells]. St. Petersburg: Publishing House of the St. Petersburg University, 2002. 388 p. (rus)
3. Rozin, L.A. Zadachi teorii uprugosti i chislennyye metody ikh resheniya [Problems of the theory of elasticity and numerical methods for their solution]. St. Petersburg: Publishing house of SPbSTU, 1998. 531 p. (rus)
4. Pikul, V.V. Mekhanika obolochek [Mechanics of shells]. Vladivostok: Dalnauka, 2009. 536 p. (rus)
5. Paimushin, V.N. On the forms of loss of stability of a cylindrical shell under an external side pressure. Journal of Applied Mathematics and Mechanics. 2016. 80 (1). Pp. 65–72.
6. Rozin, L.A., Terpugov, V.N. Variatsionnyye zadachi uprugogo ravnovesiya s odnovremenno zadannymi skachkami napryazheniy i peremeshcheniy [Variational problems of elastic equilibrium with simultaneously given jumps of stresses and displacements]. Scientific and technical statements of the St. Petersburg State Polytechnic University. 2009. 1 (74). Pp. 65–72. (rus)
7. Lalin, V.V., Zdanchuk, E.V., Kushova, D.A., Rozin, L.A. Variatsionnyye postanovki nelineynykh zadach s nezavisimymi vrashchatel'nymi stepenyami svobody [Variational formulations for non-linear problems with independent rotational degrees of freedom]. Magazine of Civil Engineering. 2015. 56(4). Pp. 54–65. (rus)
8. Postnov, V.A. Use of Tikhonov's regularization method for solving identification problem for elastic systems. Mechanics of Solids. 2010. 1 (45). Pp. 51–56.
9. Postnov, V.A., Tumashik, G.A., Moskvina, I.V. On the stability of the reinforced cylindrical shell. Strength and Ductility Problems. 2007. 69. Pp. 18–23.
10. Karpov, V., Maslennikov, A. Methods for solving non-linear tasks for calculating construction structures. World Applied Sciences Journal. 2013. 13 (23). Pp. 178–183.
11. Klochkov, Yu.V., Nikolaev, A.P., Fomin, S.D., Vakhnina, O.V., Klochkov, M.Yu. Application of volume final elements in strength calculations of engineering objects of agricultural complex. Proceedings of Lower Volga Agro-University Complex: Science and Higher Education. 2019. 4 (56). Pp. 227–237. DOI: 10.32786/2071-9485-2019-04-27
12. Magisano, D., Liang, K., Garcea, G., Leonetti, L., Ruess, M. An efficient mixed variational reduced-order model formulation for nonlinear analyses of elastic shells. International Journal for Numerical Methods in Engineering. 2018. 113 (4). Pp. 634–655.
13. Storozhuk, E.A., Maksimyuk, V.A., Chernyshenko, I.S. Nonlinear elastic state of a composite cylindrical shell with a rectangular hole. International Applied Mechanics. 2019. 55 (4). Pp. 504–514. DOI: 10.1007/s10778-019-00972-0
14. Storozhuk, E.A., Chernyshenko, I.S., Yatsura, A.V. Stress–strain state near a hole in a shear-compliant composite cylindrical shell with elliptical cross-section. International Applied Mechanics. 2018. 54 (5). Pp. 559–567. DOI: 10.1007/s10778-018-0909-8
15. Leonetti, L., Magisano, D., Madeo, A., Garcea, G., Kiendl, J., Reali, A. A simplified Kirchhoff–Love large deformation model for elastic shells and its effective isogeometric formulation. Computer Methods in Applied Mechanics and Engineering. 2019. 354. Pp. 369–396. DOI: 10.1016/j.cma.2019.05.025
16. Badriev, I.B., Paimushin, V.N. Refined Models of Contact Interaction of a Thin Plate with Positioned on Both Sides Deformable Foundations. Lobachevskii Journal of Mathematics. 2017. 38 (5). Pp. 779–793.
17. Neto, M.A., Amaro, A., Roseiro, L., Cirne, J., Leal, R. Engineering computation of structures: The finite element method. Springer, Cham. 2015. 314 p. DOI: 10.1007/978-3-319-17710-6
18. Klochkov, Yu.V., Nikolaev, A.P., Sobolevskaya, T.A., Fomin, S.D., Klochkov, M.Yu. Finite-element models of discretization of thin-walled structures of enterprises of agro-industrial complex. Proceedings of Lower Volga Agro-University Complex: Science and Higher Education. 2019. 1 (53). Pp. 255–264. DOI: 10.32786/2071-9485-2019-01-34
19. Garcea, G., Liguori, F.S., Leonetti, L., Magisano, D., Madeo, A. Accurate and efficient a posteriori account of geometrical imperfections in Koiter finite element analysis. Int. J. Numer. Methods Eng. 2017. 112 (9). Pp. 1154–1174.
20. Neto, M.A., Amaro, A., Roseiro, L., Cirne, J., Leal, R. Finite element method for plates/shells. in: engineering computation of structures: The finite element method. Springer, Cham. 2015. Pp. 195–232. DOI: 10.1007/978-3-319-17710-6_6
21. Maslennikov, A.M., Kobelev, E.A., Maslennikov, N.A. Solution of stability problems by the finite element method. Bulletin of Civil Engineers. 2020. 2(79). Pp. 68-74.
22. Lalin, V.V., Yavarov, A.V., Orlova, E.S., Gulov, A.R. Application of the finite element method for the solution of stability problems of the Timoshenko beam with exact shape functions. Power Technology and Engineering. 2019. 4(53). Pp. 449–454.

23. He, X. Finite element analysis of torsional free vibration of adhesively bonded single-lap joints. Int. J. Adhes. and Adnes. 2014. 48. Pp. 59–66.
24. Paznanova, S.L., Vasilev, G.P., Dineva, P.S., Manolis, G.D. Dynamic analysis of nanoheterogeneities in a finite-sized solidby boundary and finite element methods. Int. J. Solids and Struct. 2016. 80. Pp. 1–18.
25. Javili, A., Mc Bride, A., Steinmann, P., Reddy, B.D. A unified computational framework for bulk andsurface elasticity theory: a curvilinear-coordinate based finite element methodology. Comput. Mech. 2014. 54 (3). Pp. 745–762. DOI: 10.1007/s00466-014-1030-4
26. Nguyen, N., Waas, A.M. Nonlinear, finite deformation, finite element analysis. ZAMP. Z. Angew. Math. and Phys. 2016. 67 (3). Pp. 35/1–35/24. DOI: 10.1007/s00033-016-0623-5
27. Hansbo, P., Larson Mats G., Larson, F. Tangential differential calculus and the finite element modeling of a large deformation elastic membrane problem. Comput. Mech. 2015. 56(1). Pp. 87–95. DOI: 10.1007/s00466-015-1158-x
28. Ren, H. Fast and robust full-guad-rature triangular elements for thin plates/ shells, with large deformations and large rotations. Trans. ASME. J. Comput. and Nonlinear Dyn. 2015. 10 (5). Pp. 051018/1–051018/13.
29. Magisano, D., Liang, K., Garcea, G., Leonetti, L., Ruess, M. An efficient mixed variational reduced-order model formulation for nonlinear analyses of elastic shells. International Journal for Numerical Methods in Engineering. 2018. 113(4). Pp. 634–655.
30. Sartorato, M., De Medeiros, R., Tita, V. A finite element formulation for smart piezollectric composite shells: Mathematical formulation, computational analysis and experimental evaluation. Comros. Struct. 2015. 127. Pp. 185–198. DOI: 10.1016/j.compstruct.2015.03.009
31. Li, S., Lu, G., Wang, Z., Zhao, Longmao, Wu, G. Finite element simulatio of metallic cylindrical sandwich shells with graded aluminum tabular cores subjected to internal blast loading. Int. J. Mech. Sci. 2015. 96-97. Pp. 1–12.
32. Chi, H., Talischi, C., Lopez-Pamies, O., Paulino, G.H. A paradigm for higher order polygonal elements in finite elasticity. Comput. Methods Appl. Mech. Engrg. 2016. 306. Pp. 216–251.
33. Zucco, G., Groh, R.M.J., Madeo, A., Weaver, P.M. Mixed shell element for static and buckling analysis of variable angle tow composite plates. Compos. Struct. 2016. 152 (Suppl. C). Pp. 324–338.
34. Talischi, C., Pereira, A., Menezes, I.F., Paulino, G.H. Gradient correction for polygonal and polyhedral finite elements. Internat. J. Numer. Methods Engrg. 2015. 102 (3). Pp. 728–747. DOI: 10.1002/nme.4851
35. Manzini, G., Russo, A., Sukumar, N. New perspective on polygonal and polyhedral finite element method. Math. Models Methods Appl. Sci. 2014. 24 (08). Pp. 1665–1699. DOI: 10.1142/S0218202514400065
36. Gain, A.L., Talischi, C., Paulino, G.H. On the virtual element method for three-dimensional linear elasticity problems on arbitrary polyhedral meshes. Computer Methods in Applied Mechanics and Engineering. 2014. 282. Pp. 132–160.
37. Klochkov, Yu.V., Nikolaev, A.P., Fomin, S.D., Vakhnina, O.V., Sobolevskaya, T.A., Klochkov, M.Yu. A finite elemental algorithm for calculating the arbitrarily loaded shell using three-dimensional finite elements. ARPN Journal of Engineering and Applied Sciences. 2020. 15(13). Pp. 1472–1481.
38. Beirao da Veiga, L., Lovadina, C., Mora, D. A virtual element method for elastic and inelastic problems on polytope meshes. Comput. Methods Appl. Mech. Engrg. 2015. 295. Pp. 327–346.
39. Antonietti, P.F., Beirao da Veiga, L., Scacchi, S., Verani, M. A C1 Virtual element method for the Cahn–Hilliard equation with polygonal meshes. SIAM J. Numer. Anal. 2016. 54 (1). Pp. 34–56.
40. Klochkov, Yu.V., Nikolaev, A.P., Sobolevskaya, T.A., Vakhnina, O.V., Klochkov, M.Yu. The calculation of the ellipsoidal shell based FEM with vector interpolation of displacements when the variable parameterisation of the middle surface. Lobachevskii Journal of Mathematics. 2020. 41 (3). Pp. 373–381. DOI: 10.1134/S1995080220030117
41. Pogorelov, A.V. Differentsial'naya geometriya [Differential geometry]. 6th ed., stereotype. Moscow: Nauka, 1974. 176 p. (rus)
42. Sedov, L.I. Mekhanika sploshnoy sredy [Mechanics of a continuous medium]. v. 1. Moscow: Nauka, 1976. 536 p. (rus)
43. Zubchaninov V.G. Ustoychivost' i plastichnost'. Tom 2. Plastichnost' [Stability and plasticity. Volume 2. Plasticity]. Moscow: Fizmatlit, 2007. 336 p. (rus)
44. Chi, H., Beirãoda Veiga L., Paulino, G.H. Some basic formulations of the virtual element method (VEM) for finite deformations. Comput. Methods Appl. Mech. Engrg. 2017. 318. Pp. 148–192.
45. Roehl, D., Ramm, E. Large elasto-plastic finite element analysis of solids and shells with the enhanced assumed strain concept. International Journal of Solids and Structures. 1996. 33. Pp. 3215–3237.


### *Contacts:*


***Yury Klochkov,***
*Doctor of Technical Science*
*ORCID: https://orcid.org/0000-0002-1027-1811*
*E-mail: Klotchkov@bk.ru*

***Anatoliy Nikolaev,***
*Doctor of Technical Science*
*ORCID: https://orcid.org/0000-0002-7098-5998*
*E-mail: anpetr40@yandex.ru*

***Olga Vakhnina,***
*PhD of Technical Science*
*ORCID: https://orcid.org/0000-0001-9234-7287*
*E-mail: ovahnina@bk.ru*

***Tatyana Sobolevskaya,***
*PhD of Technical Science*
*ORCID: https://orcid.org/0000-0002-9167-075X*
*E-mail: moonway13@rambler.ru*

***Michael Klochkov,***
*E-mail: m.klo4koff@yandex.ru*

*Received 29.04.2021. Approved after reviewing 15.11.2021. Accepted 19.11.2021.*